6-2009

Disruption of OsYSL15 Leads to Iron Inefficiency in Rice Plants

Sichul Lee
Pohang University of Science and Technology

Jeff C. Chiecko
University of Massachusetts,Amherst

Sun A. Kim
Dartmouth College

Elsbeth L. Walker
University of Massachusetts,Amherst

Youngsook Lee
Pohang University of Science and Technology

See next page for additional authors

Disruption of *OsYSL15* Leads to Iron Inefficiency in Rice Plants[1][C][W][OA]

Sichul Lee, Jeff C. Chiecko, Sun A. Kim, Elsbeth L. Walker, Youngsook Lee, Mary Lou Guerinot, and Gynheung An*

Department of Integrative Bioscience and Biotechnology, Pohang University of Science and Technology, Pohang 790–784, Republic of Korea (S.L., Y.L., G.A.); Department of Biology, University of Massachusetts, Amherst, Massachusetts 01003 (J.C.C., E.L.W.); and Department of Biological Sciences, Dartmouth College, Hanover, New Hampshire 03755 (S.A.K., M.L.G.)

Uptake and translocation of metal nutrients are essential processes for plant growth. Graminaceous species release phytosiderophores that bind to Fe^{3+}; these complexes are then transported across the plasma membrane. We have characterized *OsYSL15*, one of the rice (*Oryza sativa*) *YS1-like* (*YSL*) genes that are strongly induced by iron (Fe) deficiency. The *OsYSL15* promoter fusion to *β-glucuronidase* showed that it was expressed in all root tissues when Fe was limited. In low-Fe leaves, the promoter became active in all tissues except epidermal cells. This activity was also detected in flowers and seeds. The OsYSL15:green fluorescent protein fusion was localized to the plasma membrane. OsYSL15 functionally complemented yeast strains defective in Fe uptake on media containing Fe^{3+}-deoxymugineic acid and Fe^{2+}-nicotianamine. Two insertional *osysl15* mutants exhibited chlorotic phenotypes under Fe deficiency and had reduced Fe concentrations in their shoots, roots, and seeds. Nitric oxide treatment reversed this chlorosis under Fe-limiting conditions. Overexpression of *OsYSL15* increased the Fe concentration in leaves and seeds from transgenic plants. Altogether, these results demonstrate roles for OsYSL15 in Fe uptake and distribution in rice plants.

Iron (Fe), an essential nutrient for plants, plays a crucial role in a variety of cellular functions. Because plants are the primary source of food for humans, their nutritional value is important to health. The most widespread dietary problem in the world is Fe deficiency (World Health Organization, 2003). Such a deficiency also causes a metabolic imbalance deleterious to plant growth (e.g. impairing chlorophyll biosynthesis, chloroplast development, and photosynthesis). Therefore, Fe availability is directly correlated with plant productivity.

Despite its abundance in soils, Fe is present as oxihydrates with low bioavailability. To avoid a deficiency, two distinct strategies are possible for Fe acquisition (Marschner et al., 1986). In strategy I, used by dicotyledonous and nongraminaceous monocotyledonous plants, Fe^{2+} transport is coupled to an Fe^{3+} chelate reduction step. Under Fe deficiency, protons are released via H^+-ATP pumps into the rhizosphere to lower the soil pH, and subsequently, Fe^{3+}-chelate reductase is induced to reduce Fe^{3+} to the more soluble Fe^{2+}, which is then absorbed by a specific transporter. The plasmalemma root ferric-chelate reductase, FRO2, reduces soil Fe^{3+} (Robinson et al., 1999) and provides Fe^{2+} for IRT1, a major metal transporter that takes up Fe^{2+} into the root epidermis. This is evidenced by the lethal chlorotic phenotypes of *IRT1* knockout mutants (Eide et al., 1996; Henriques et al., 2002; Varotto et al., 2002; Vert et al., 2002).

With strategy II, low Fe availability in the soil is overcome in grasses such as maize (*Zea mays*) and rice (*Oryza sativa*). In response to Fe deficiency, these crops synthesize and release nonproteinogenic amino acids in the mugineic acid family of phytosiderophores (MAs) to fix Fe^{3+} in the soil (Takagi et al., 1984). All MAs are synthesized from L-Met, sharing the same pathway from L-Met to 2′-deoxymugineic acid (DMA; Bashir et al., 2006). L-Met is adenosylated by *S*-adenosylmethionine synthetase (Takizawa et al., 1996). Nicotianamine synthase (NAS) catalyzes the trimerization of *S*-adenosylmethionine molecules to form nicotianamine (NA; Higuchi et al., 1999), which is then

[1] This work was supported by the Crop Functional Genomic Center, 21st Century Frontier Program (grant no. CG1111), the Biogreen 21 Program of the Rural Development Administration (grant no. 20070401–034–001–007–03–00), the National Research Laboratory Program of the Ministry of Science and Technology (grant no. M10600000270–06J0000–27010), the U.S. Department of Agriculture National Research Initiative Competitive Grants Program (grant no. 2005–01072 to E.L.W.), and the National Science Foundation (grant no. DB10701119 to M.L.G.).

* Corresponding author; e-mail genean@postech.ac.kr.

The author responsible for distribution of materials integral to the findings presented in this article in accordance with the policy described in the Instructions for Authors (www.plantphysiol.org) is: Gynheung An (genean@postech.ac.kr).

[C] Some figures in this article are displayed in color online but in black and white in the print edition.

[W] The online version of this article contains Web-only data.

[OA] Open Access articles can be viewed online without a subscription.

www.plantphysiol.org/cgi/doi/10.1104/pp.109.135418

converted into a 3″-keto intermediate via the transfer of an amino group by nicotianamine aminotransferase (NAAT; Inoue et al., 2008). Genes encoding NAS and NAAT for MA biosynthesis have been isolated (Higuchi et al., 1999; Takahashi et al., 1999; Inoue et al., 2003, 2008). The subsequent reduction of the 3″-carbon in the keto intermediate produces DMA by DMA synthase (Bashir et al., 2006). In response to Fe deficiency, these grasses increase their production and secretion of MAs into the rhizosphere, where they chelate various metals, including Fe^{3+}. The Fe^{3+}-MA complexes are then taken up by an Fe^{3+}-MA transporter. The *Yellow Stripe1* (*YS1*) gene has been isolated and characterized in maize, where it encodes the high-affinity Fe^{3+}-MA transporter (Curie et al., 2001). YS1 functions as a proton-coupled symporter for phytosiderophore (PS)-chelated metals (Curie et al., 2001; Roberts et al., 2004; Schaaf et al., 2004).

Among the 18 *YS1-like* (*YSL*) genes in rice, *OsYSL2* is up-regulated by Fe deficiency in the leaves, particularly in the phloem, and is also expressed in developing seeds (Koike et al., 2004). OsYSL2:GFP is localized to the plasma membrane. Electrophysiological measurements using *Xenopus laevis* oocytes have shown that OsYSL2 transports Fe^{2+}-NA and Mn^{2+}-NA but not Fe^{3+}-DMA (Koike et al., 2004). OsYSL15 encodes a functional Fe^{3+}-DMA transporter whose expression pattern strongly indicates its involvement in Fe^{3+}-DMA uptake from the rhizosphere and in phloem transport of Fe (Inoue et al., 2009). *OsYSL15* knockdown seedlings are severely arrested in their germination and early growth but are rescued by a high Fe supply, demonstrating that OsYSL15 plays a crucial role in Fe homeostasis during the first stages of growth (Inoue et al., 2009). It is generally believed that most plants depend largely on a single strategy (I or II) for Fe acquisition. In graminaceous plants, such as barley (*Hordeum vulgare*) and maize, the inducible Fe^{2+} transporter system either is absent or is expressed at very low levels (Zaharieva and Romheld, 2001). Rice and its wild relatives are well adapted for growth under submerged conditions, in which Fe^{2+} is more abundant than Fe^{3+}. Isolation of *OsIRT1* and *OsIRT2*, which encode functional Fe^{2+} transporters (Bughio et al., 2002; Ishimaru et al., 2006), suggests that rice plants can take up Fe^{2+} even though they do not have inducible Fe^{2+} chelate reductase activity (Ishimaru et al., 2006). Analysis with the positron-emitting tracer imaging system has confirmed that, in addition to taking up Fe^{3+}-DMA, rice plants can absorb Fe^{2+} from the root environment (Ishimaru et al., 2006).

The presence of *YSL* genes is not restricted to strategy II plants. In fact, eight orthologs (*AtYSL1*–*AtYSL8*) have been found in *Arabidopsis* (Curie et al., 2001), a genus that neither synthesizes nor uses MAs. NA is the biosynthetic precursor to MAs and is also a strong chelator of various transition metals (von Wirén et al., 1999). NA is ubiquitous in the plant kingdom, and these YSL proteins mediate the internal transport of metals bound to NA (Walker, 2002). *AtYSL1* is a shoot-specific gene whose transcript levels increase in response to high-Fe conditions (Le Jean et al., 2005). It is also expressed in young siliques, suggesting a role in the Fe loading of seeds. Indeed, mutations in that gene reduce seed Fe content and delay germination, but those can be rescued by exogenous Fe. *AtYSL2* transcript levels are decreased under Fe-deficient conditions; they also respond to copper (Cu) and zinc (Zn; DiDonato et al., 2004; Schaaf et al., 2005). Whereas single mutants of *ysl1* and *ysl3* have no visible phenotypes, the *ysl1/ysl3* double mutants exhibit Fe deficiency symptoms. Likewise, their mobilization of Zn and Cu from the leaves is impaired during senescence, suggesting that the physiological roles for YSL1 and YSL3 are their delivery of metal micronutrients to and from vascular tissues (Waters et al., 2006). In the heavy-metal hyperaccumulator *Thlaspi caerulescens*, *TcYSL3*, a member of the *YSL* gene family, encodes a Ni/Fe-NA transporter (Gendre et al., 2007).

Nitric oxide (NO) is a bioactive molecule implicated in a number of physiological functions, including the intracellular and intercellular mediation of some animal responses (Anbar, 1995). It also serves as a cellular messenger in controlling growth, development, and adaptive responses to multiple stresses in higher plants (Durner and Klessig, 1999; Beligni and Lamattina, 2001; Neill et al., 2002; Lamattina et al., 2003; Graziano and Lamattina, 2005; Lopez-Bucio et al., 2006). NO stimulates the accumulation of both ferritin mRNA and protein, suggesting that it is a signaling molecule for modulating Fe homeostasis in plants (Murgia et al., 2002). NO probably acts through the regulation of a trans-acting factor, because its effect relies on the Fe-dependent regulatory sequence present on the *Atfer1* promoter. NO appears to play a role in improving Fe availability within a plant, as demonstrated by an Fe-deficiency phenotype that is recovered by NO without changing the internal levels of total Fe (Graziano et al., 2002). In tomato (*Solanum lycopersicum*), the NO level is increased in deprived roots to improve Fe availability by controlling the expression of uptake-related genes and by regulating the physiological and morphological adaptive responses to Fe-deficient conditions (Graziano and Lamattina, 2007).

Here, we have determined the physiological roles of *OsYSL15* in Fe homeostasis using two independent T-DNA insertional mutants and overexpression lines.

RESULTS

Expression Analysis of *OsYSL* Genes under Different Fe Concentrations

Rice has 18 putative *OsYSL* genes (Koike et al., 2004). Among them, *OsYSL2*, *OsYSL9*, *OsYSL15*, and *OsYSL16* are phylogenetically grouped with maize *YS1* (Koike et al., 2004). We used quantitative real-time PCR to investigate whether expression of these four rice genes is responsive to changes in the external Fe

supply (Fig. 1). Seedlings were grown for 7 d on Murashige and Skoog (MS) medium with 0, 1, 10, 100, or 500 μM Fe. Standard MS medium contains 100 μM Fe. At the highest concentration, transcript levels were similar to those measured in plants grown on the standard. However, when Fe was limited, transcripts of *OsYSL2*, *OsYSL9*, and *OsYSL15* were increased. The degree of induction was greater in shoots than in roots. In contrast, a reduction in Fe concentration did not significantly affect the expression of *OsYSL16*. Previous analysis with northern blots showed that *OsYSL15* transcripts are not detected in the leaves of Fe-deficient rice plants (Koike et al., 2004; Inoue et al., 2009). This experimental inconsistency may have been due to differences in growing conditions, age of the plants, and genetic background. Here, we germinated rice seeds on agar medium containing different Fe concentrations and then grew the seedlings for 7 d prior to sampling. In contrast, Koike et al. (2004) and Inoue et al. (2009) reared their seedlings on an Fe-sufficient nutrient medium for 3 weeks, then transferred the plants to an Fe-deficient solution for 3 more weeks before sampling. Therefore, it is possible that their plants were not fully Fe limited at the sampling time. Furthermore, we used a different rice cultivar (Dongjin) whose genetic variation may have affected *OsYSL15* expression under Fe deficiency. However, the expression of *OsYSL2*, which was induced by Fe deficiency in root and shoots, was similar to that described in a previous report (Koike et al., 2004).

We also tested the expression of the other 14 *OsYSL* genes at different Fe concentrations. The expression of *OsYSL5*, *OsYSL6*, *OsYSL12*, *OsYSL13*, and *OsYSL14* was relatively constant irrespective of Fe status (Supplemental Fig. S1). By comparison, no expression of *OsYSL1*, *OsYSL3*, *OsYSL4*, *OsYSL7*, *OsYSL8*, *OsYSL10*, *OsYSL11*, *OsYSL17*, or *OsYSL18* was observed under our experimental conditions.

Expression Analysis of *OsYSL15* Using the Promoter-GUS Fusion Molecule

To investigate the spatial and temporal expression patterns of *OsYSL15*, we generated transgenic plants carrying the 1.0-kb *OsYSL15* promoter region that was fused to the *uidA* reporter gene. Histochemical GUS staining of 5-d-old seedlings showed that GUS activity was stronger in seedlings grown under Fe-deficient conditions (Fig. 2A, right) than in those in an Fe-sufficient scenario (Fig. 2A, left). Cross sections of the seminal roots cultured under the latter exhibited activity that was present mainly in the vascular cylinder (Fig. 2B). In response to Fe deficiency, GUS activity increased throughout the root tissues, including epidermis, exodermis, endodermis, cortex, and vascular cylinder (Fig. 2C). In leaves, activity was hardly detectable when the plants were grown on an Fe-supplemented medium (Fig. 2, D and F). When Fe was deficient, the *OsYSL15* promoter became active in all tissues except the epidermal cells, suggesting a role for OsYSL15 in Fe distribution within the leaves (Fig. 2, E and G). These observations coincide with our previous results from quantitative real-time PCR analysis (Fig. 1C). However, results from our promoter-*GUS* analysis contrast with those previously reported by Inoue et al. (2009), where the *OsYSL15* promoter was weakly

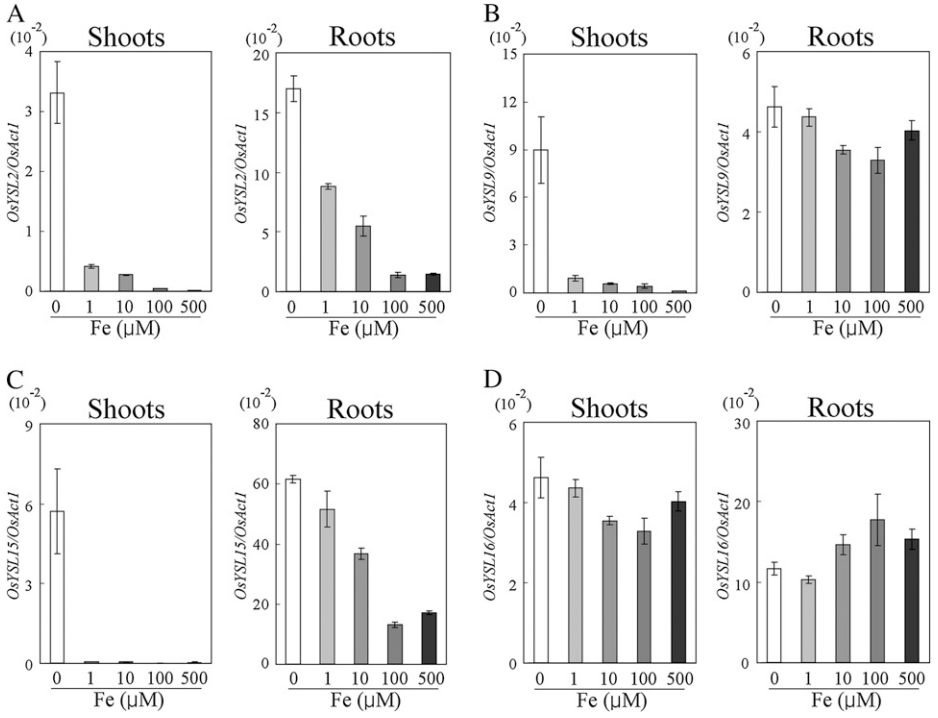

Figure 1. Real-time PCR analysis of *OsYSL* genes under different Fe concentrations. Seedlings were grown for 7 d on MS medium containing 0, 1, 10, 100, or 500 μM Fe. Each value is the average of three independent experiments. Transcript levels are represented by the ratio between mRNA levels of *OsYSL2* (A), *OsYSL9* (B), *OsYSL15* (C), and *OsYSL16* (D) and those of rice *Actin1*. The nomenclature of *OsYSL* genes in this study is the same as presented by Koike et al. (2004). Error bars indicate SD. Gene-specific primers are listed in Supplemental Table S2.

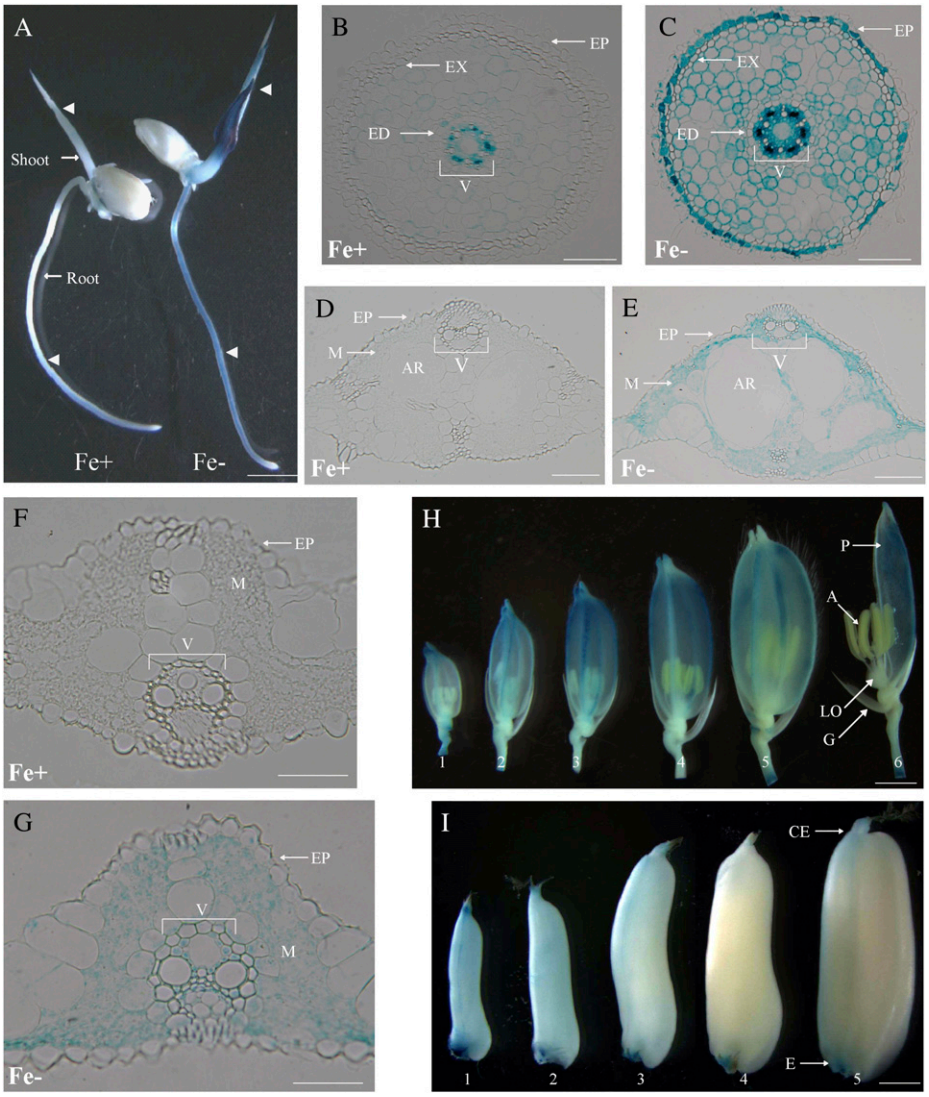

Figure 2. Spatial expression patterns of the *OsYSL15-GUS* construct. A, Five-day-old seedlings grown on Fe-sufficient (Fe+) or Fe-deficient (Fe−) medium. B, Cross section of a 5-d-old seedling root grown under Fe-sufficient conditions. The analyzed region is at the differentiation zone (arrowhead in A). C, Cross section of a 5-d-old seedling root grown on Fe-deficient medium. The analyzed region is at the differentiation zone (arrowhead in A). D and E, Cross sections of midrib regions from leaves under Fe-sufficient (D) or Fe-deficient (E) conditions. The analyzed regions are indicated as arrowheads in A. F and G, GUS expression in leaf blades under Fe-sufficient (F) or Fe-deficient (G) conditions. H, Temporal and spatial expression patterns of *OsYSL15-GUS* fusion in spikelets at various developmental stages. Samples are as follows: 1, tetrad; 2, early young microspore; 3, late young microspore; 4, vacuolated pollen; 5, late pollen mitosis; 6, dehulled flower at late pollen mitosis stage. I, GUS activity in developing seeds at various stages. Samples are as follows: 1, 3 d after pollination (DAP); 2, 5 DAP; 3, 7 DAP; 4, 10 DAP; 5, 20 DAP. A, Anther; AR, aerenchyma; C, cortex; CE, chalazal end; E, embryo; ED, endodermis; EP, epidermis; EX, exodermis; G, glume; LO, lodicules; M mesophyll; P, palea; V, vascular bundle. Bars = 0.5 cm in A, 50 μm in B to G, 1 mm in H, and 0.5 mm in I.

active in companion cells and in some of the xylem parenchyma of Fe-sufficient leaves. Fe deficiency treatment did not change expression levels or localization. In our experiments, we used 5-d-old seedling plants grown in sufficient or deficient medium to determine *OsYSL15* promoter activity. By comparison, Inoue et al. (2009) used 6-week-old plants to analyze GUS expression. This difference may explain these contradictory results.

Because reproductive organs are the major sinks for Fe, we examined *OsYSL15* expression in the flowers and seeds. In the developing spikelets, GUS activity was detectable mainly in the vascular bundles of the palea and lemma but not in the lodicule, anther, and ovary (Fig. 2H). After pollination, activity was found in the upper part of the carpel, including the style and stigma, and also in the embryo (Fig. 2I). During seed development, GUS expression remained unchanged, suggesting that OsYSL15 also functions in the translocation of Fe into rice grains.

OsYSL15 Is a Plasma Membrane-Localized Transporter

To determine the subcellular localization of OsYSL15, we prepared a DNA construct containing a fusion between *OsYSL15* and *GFP* (Fig. 3). This *OsYSL15-GFP* construct was expressed transiently in onion (*Allium cepa*) epidermal cells. The PSORT program (http://psort.nibb.ac.jp) predicted that OsYSL15 would localize to the plasma membrane with high probability. We also used a control construct, which expressed a fusion protein between red fluorescent protein (RFP) and the Arabidopsis (*Arabidopsis thaliana*) proton ATPase2 (AHA2) that is localized to the plasma membrane (Fig. 3A; Kim et al., 2001). The DNA constructs, encoding OsSYL15-GFP and AHA2-RFP under the control of the cauliflower mosaic virus *35S* promoter, were simultaneously delivered via particle bombardment (Fig. 3B). After 12 h of incubation, expression of the introduced genes was examined with a fluorescence microscope. The green fluorescent signal was

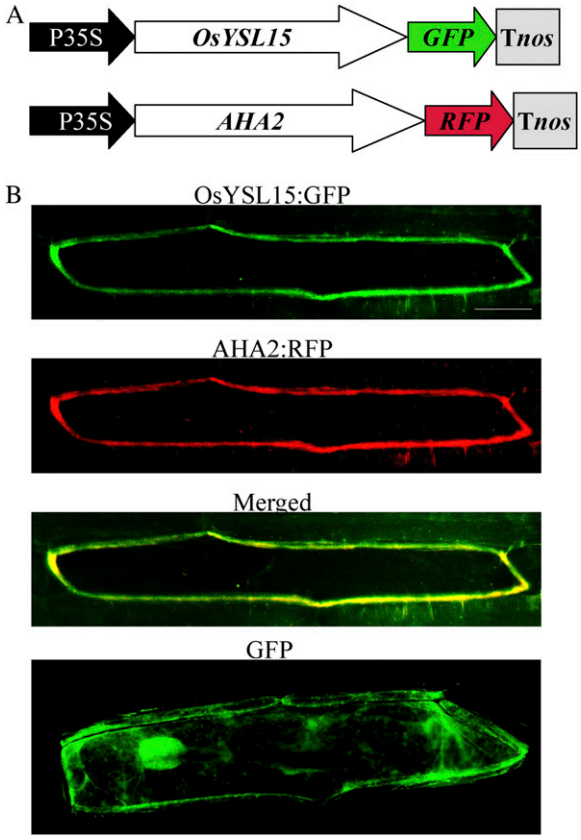

Figure 3. Subcellular localization of OsYSL15:GFP in onion epidermal cells. A, Schematic diagrams of fusion constructs. P35S, Cauliflower mosaic virus *35S* promoter; T*nos, nopaline synthase* gene terminator. B, Onion cells cotransformed with OsYSL15:GFP and AHA2:RFP fusion constructs via particle bombardment. Fluorescent signals were examined 12 h after transfection. Data are representative of transformed cells. At least two independent transformation experiments were performed with each construct. "Merged" indicates that green and red signals were merged. Expression of GFP alone was analyzed as a control. Bar = 25 μm.

detected at the plasma membrane coincident with the red signal driven by the AHA2-RFP (Fig. 3B). When GFP alone was expressed as a control, the protein was localized in the cytoplasm and nucleus (Fig. 3B). These results suggest that OsYSL15 is located at the plasma membrane.

Transporter Activity of OsYSL15

We tested whether OsYSL15 is capable of transporting Fe using the *fet3fet4* yeast strain that is defective in Fe uptake (Dix et al., 1994). In this assay, the mutant strain was transformed with either the *OsYSL15*-expressing plasmid or the empty *pYES6/CT* vector, which served as a negative control. We utilized a β-estradiol-regulated expression system to control the level of *OsYSL15* expression in yeast (Gao and Pinkham, 2000). Via this system, we achieved a tightly regulated off state. Viability of the strains was proved by growing them under permissive conditions (50 μM Fe citrate; Fig. 4, A and G). To examine whether OsYSL15 can transport Fe^{3+}, the strain containing the vector alone or else *OsYSL15* was grown on a medium with $FeCl_3$ (Fig. 4B) or on one with $FeCl_3$ plus DMA (Fig. 4C). This experiment showed that OsYSL15 complemented yeast growth in the presence of $FeCl_3$ and DMA but not with $FeCl_3$ alone, thereby suggesting that OsYSL15 is able to transport Fe-PS complexes. When β-estradiol was withheld from the medium, the strain was unable to grow, demonstrating its dependence upon *OsYSL15* expression (Fig. 4D). Functional complementation still occurred when a strong Fe^{2+} chelator, 4,7-biphenyl-1,10-phenanthroline-disulfonic acid (BPDS), was used to remove any residual Fe^{2+} from the Fe^{3+}-DMA medium (Fig. 4E), thus supporting that OsYSL15 transports Fe^{3+}.

When Fe^{2+} was provided as $FeSO_4$, OsYSL15 failed to restore growth (Fig. 4H), but when NA was added along with $FeSO_4$, OsYSL15 complemented *fet3fet4* (Fig. 4I). Growth of the strain depended on the presence of β-estradiol (Fig. 4J). These results indicate that OsYSL15 is capable of utilizing both Fe^{2+}-NA and Fe^{3+}-DMA.

Disruption of *OsYSL15* Results in Chlorotic Phenotypes under Fe Deficiency

To examine the role of OsYSL15 further, we isolated mutants in which the *OsYSL15* gene was disrupted. From our rice flanking sequence tag database (An et al., 2003; Jeong et al., 2006), we identified two independent T-DNA knockout alleles. T-DNA was inserted into the second intron and second exon in *osysl15-1* and *osysl15-2*, respectively (Fig. 5A). T2 progeny were genotyped by PCR to obtain homozygous knockout plants and segregated wild-type siblings using gene-specific primers and a T-DNA primer (Fig. 5A). Reverse transcription (RT)-PCR analysis revealed the disruption of *OsYSL15* expression in T-DNA homozygous plants, demonstrating that both are null alleles (Fig. 5B).

To study the roles of OsYSL15 in Fe transport, we germinated seeds of the *osysl15* homozygous progeny and their wild-type segregants, then grew their seedlings on solid MS medium in the absence or presence of Fe (100 μM). When they were supplied with a sufficient amount of micronutrients in the control MS medium, the mutant plants did not differ in phenotype from the wild-type segregants (Fig. 5C). Growth rates, based on heights and fresh weights, also did not vary significantly between the two (Supplemental Fig. S2, A and B), and chlorophyll concentrations in the knockout plants were not significantly different from that of the wild type (Supplemental Fig. S2C). However, the *osysl15* mutants showed impaired growth on the Fe-deficient medium (Fig. 5D), differing from the wild type in their heights, fresh weights, and total chlorophyll concentration (Supplemental Fig. S2). For

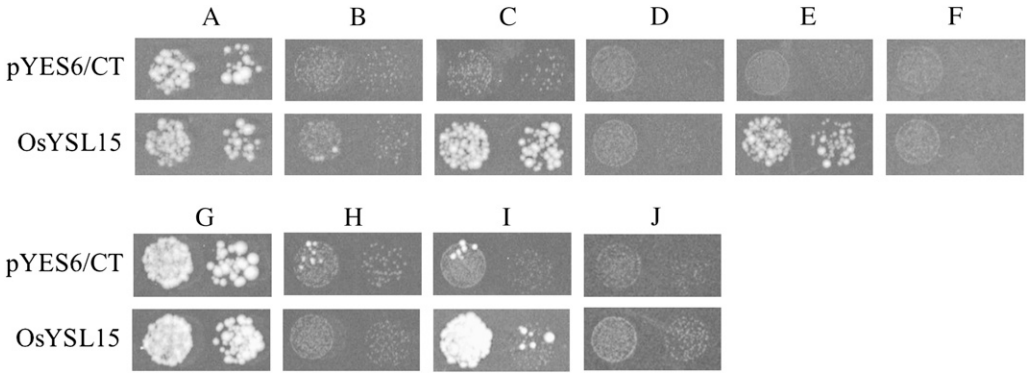

Figure 4. Functional complementation of *fet3fet4* yeast. DEY1453-derived yeast strains transformed with pGEV-TRP and constructs expressing *OsYSL15* or empty *pYES6/CT* were grown on synthetic defined medium containing 50 μM Fe citrate (A and G); 10 μM $FeCl_3$ with 40 nM β-estradiol (B); 10 μM $FeCl_3$ with 10 μM DMA and 40 nM β-estradiol (C); 10 μM $FeCl_3$ with 10 μM DMA without β-estradiol (D); 10 μM $FeCl_3$ with 10 μM DMA, 10 μM BPDS, and 40 nM β-estradiol (E); 10 μM $FeCl_3$, 10 μM DMA, and 10 μM BPDS without β-estradiol (F); 3 μM $FeSO_4$ with 10 nM β-estradiol (H); 3 μM $FeSO_4$ with 8 μM NA and 10 nM β-estradiol (I); or 3 μM $FeSO_4$ with 8 μM NA without β-estradiol (J). Pairs of spots correspond to 10-fold and 100-fold dilutions of original cultures.

example, respective heights for *osysl15-1* and *osysl15-2* were reduced to 63% and 69%, fresh weights to 78% and 77%, and chlorophyll concentrations to 54% and 57%, relative to the wild type. We also tested the growth of knockout plants under Zn deficiency and found no distinction between the *osysl15* knockout mutants and the wild type in their appearance, fresh weights, and chlorophyll concentrations (Fig. 5E; Supplemental Fig. S2). These results are contradictory to the ones from *OsYSL15* knockdown seedlings grown in the standard MS medium, which showed severe arrest in germination and early growth and died less than 21 d after sowing (Inoue et al., 2009). This discrepancy may have been caused by different genetic backgrounds, resulting in a variation in sensitivity to Fe deficiency between rice cultivars.

To evaluate whether the disruption of *OsYSL15* affects Fe distribution, we measured Fe concentrations in shoots and roots at the seedling stage. When plants were grown in an Fe-sufficient medium, concentrations from *osysl15-1* and *osysl15-2* were reduced to 79% and 77% that of the wild type in the shoots and to 84% and 84% that of the wild type in the roots (Fig. 6A). Under Fe deficiency, relative concentrations in *osysl15-1* and *osysl15-2* also were decreased to 79% and 75% in shoots and to 78% and 79% in roots, respectively (Fig. 6A). However, Zn concentrations in *osysl15-1* and *osysl15-2* were not significantly different from those in the wild-type plants (Fig. 6B). Levels of Cu and manganese (Mn) were also unchanged in shoots and roots (Supplemental Fig. S3, A and B).

Whereas Fe concentrations in *osysl15* mutants were reduced to 80% of normal, their chlorophyll concentrations were decreased to 50% that of the wild type under Fe deficiency. To evaluate Fe distribution in plants, we measured Fe concentrations in mesophyll protoplasts and chloroplasts from 10-d-old wild-type and *osysl15-1* seedlings (Fig. 6, C and D). Under both sufficient and deficient conditions, concentrations in the protoplasts were reduced to 80% in *osysl15-1* compared with the wild type. Whereas the Fe concentration from *osysl15-1* chloroplasts was reduced to 80% that of wild-type chloroplasts under Fe sufficiency, the concentration from *osysl15-1* chloroplasts was only 66% that of wild-type chloroplasts under Fe deficiency. This was consistent with the severe chlorosis of *osysl15-1* under Fe deficiency. However, Zn levels in the chloroplasts were not affected by disruption of *OsYSL15* (data not shown).

Promoter-GUS analysis showed that *OsYSL15* was also active during seed development. Therefore, we postulated that disruption of *OsYSL15* would affect Fe loading into the grains. In fact, those from *osysl15-1* and *osysl15-2* had 83% and 87% as much Fe, respectively, as seeds measured from the wild type (Fig. 6E), while Zn concentrations were similar for both homozygous knockout plants and the wild type (Fig. 6F). Levels of Cu and Mn were unchanged in mature seeds (Supplemental Fig. S3, C and D).

Effect of NO on Reversing the Chlorotic Phenotype of *osysl15*

NO is able to reverse the chlorotic phenotypes of two Fe-inefficient maize mutants, *ys1* and *ys3*, both impaired in their Fe uptake (Graziano et al., 2002). Because our *osysl15* mutants also showed a chlorotic phenotype in response to Fe deficiency, we evaluated whether NO could likewise rescue the deficiency symptoms of the mutants. Rice seeds were germinated and seedlings were grown for 10 d on Fe-deficient media containing various concentrations of sodium nitroprusside (SNP), an NO donor. NO-mediated increases in chlorophyll concentration were more prom-

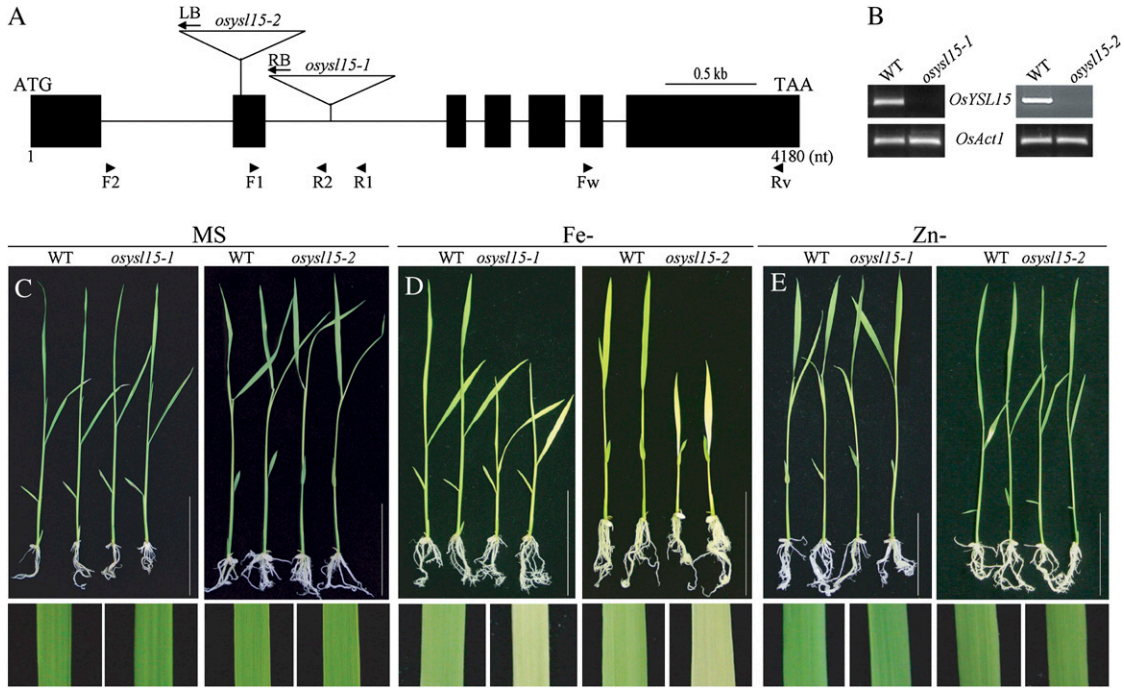

Figure 5. Isolation and characterization of *OsYSL15* knockout mutant plants. A, Schematic diagram of *OsYSL15* and insertion positions of T-DNA. Black boxes indicate seven exons, and connecting black lines represent introns. In line 2D10712, T-DNA was inserted into the second intron (*osysl15-1*) of *OsYSL15*; in line 3A10357, DNA was inserted into the second exon (*osysl15-2*) of *OsYSL15*. Horizontal arrowheads indicate primers (F1, R1, F2, and R2) used for genotyping T2 progeny. LB, Left border; RB, right border. B, RT-PCR analyses of *OsYSL15* expression. *OsYSL15*-specific primers (Fw and Rv) were used with total RNA from leaves of *osysl15-1*, *osysl15-2*, or segregated wild-type (WT) seedlings grown under Fe deficiency. Rice *Actin1* (*OsAct1*) was amplified as an internal control. C to E, Phenotype analyses of *OsYSL15* knockout plants at seedling stage under Fe and Zn deficiencies. Homozygous and wild-type progeny of *osysl5-1* and *osysl15-2* were germinated and grown for 10 d on solid MS medium in the presence of Fe (100 μM) and Zn (30 μM) or in the absence of Fe (Fe−) or Zn (Zn−). Bottom panels show enlargements of second leaves. C, Wild-type and knockout mutant plants grown on MS control medium. D, Wild-type and knockout mutant plants grown on Fe-deficient medium. E, Wild-type and knockout mutant plants grown on Zn-deficient medium. Photographs were taken 10 d after germination. Bars = 5 cm. [See online article for color version of this figure.]

inent in *osysl15-1* than in wild-type plants (Fig. 7A; Supplemental Fig. S4C). Although 10 μM SNP was effective in elevating chlorophyll levels in the wild type, 50 μM SNP was needed to reverse chlorophyll deficiencies in the mutant (Fig. 7C).

We evaluated the effect of NO depletion using an NO-specific scavenger, 2-(4-carboxy-phenyl)-4,4,5,5-tetramethyllimidazoline-1-oxyl-3-oxide (CPTIO). Treatment with 100 μM CPTIO almost abolished the protective effect of NO on plant growth and chlorophyll accumulation in *osysl15-1* mutants (Fig. 7, A and C; Supplemental Fig. S4). The chlorophyll concentration was reduced to 83% in treated plants compared with untreated mutants. However, CPTIO had no effect on wild-type plants (Fig. 7). Under Fe-sufficient conditions, CPTIO did not influence seedling growth in either the wild type or the mutant.

NO treatment did not change the whole plant Fe concentration or enhance translocation of Fe from one organ to another (Supplemental Fig. S4D). Our results are consistent with the previous suggestion that NO improves the internal availability of Fe.

Expression Analysis of Fe Homeostasis-Related Genes in *osyls15-1*

NO plays a role in many different signaling pathways and affects the expression of numerous genes. To evaluate its influence on Fe homeostasis, we examined three *NAS* genes and two *ferritin* genes. Transcript levels of *OsNAS1* and *OsNAS2* were not detectable when Fe was sufficient but were markedly increased in response to Fe deficiency (Fig. 8A). In wild-type plants, NO treatment abolished gene expression even at a low dose (i.e. 10 μM SNP). In the *osysl15-1* mutant, however, expression of those two genes could be detected even when 25 μM SNP was supplied (Fig. 8A). Under NO treatment, CPTIO induced their expression in the mutants but not in the wild type (Fig. 8B). *OsNAS3* was expressed in plants grown on an Fe-sufficient medium but was suppressed when Fe was limited. NO treatment upon Fe deficiency increased *OsNAS3* expression in both wild-type and mutant plants (Fig. 8A), although to a relatively lesser extent in the latter.

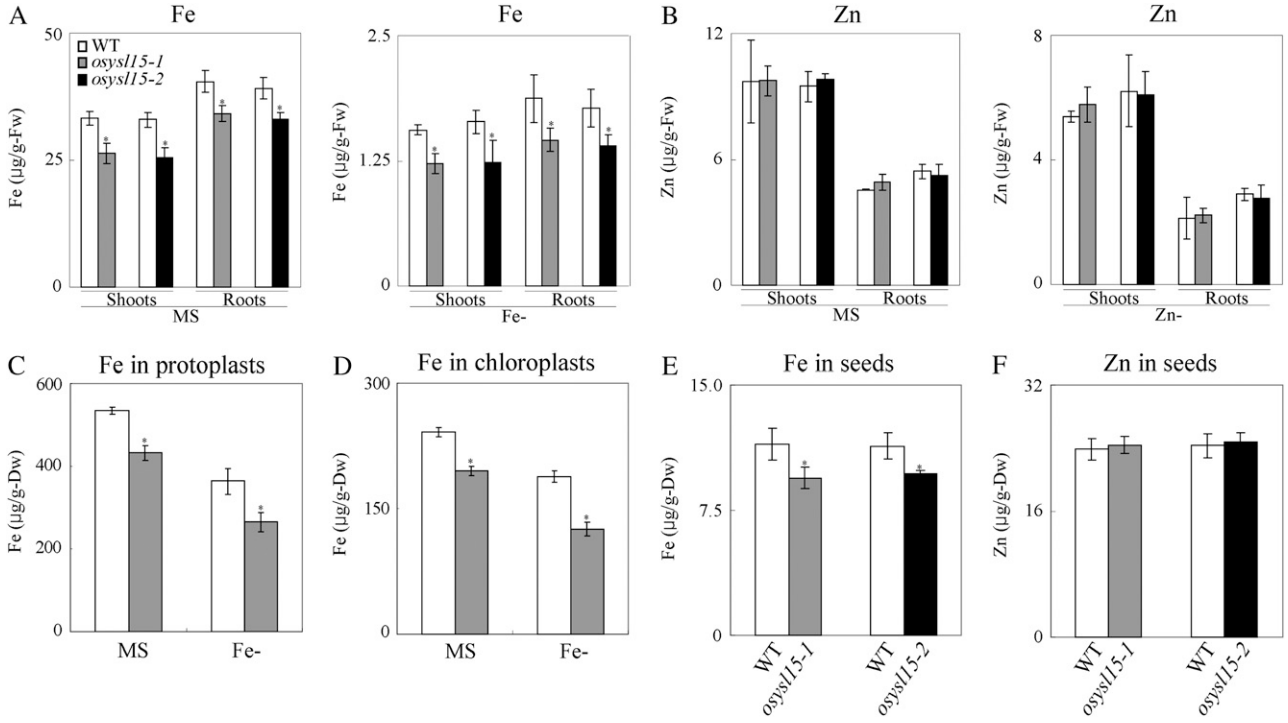

Figure 6. A and B, Fe (A) and Zn (B) concentrations in shoots and roots from wild-type (WT) and *osysl15* mutant plants grown on standard MS, Fe-deficient (Fe−), or Zn-deficient (Zn−) medium. At least two independent experiments were conducted for metal measurements, each using four plants. C and D, Fe concentrations in protoplasts and chloroplasts from wild-type and *osysl15-1* plants grown on standard MS or Fe-deficient (Fe−) medium. E, Fe concentration in seeds from paddy-grown plants. F, Zn concentration in 10 pooled seeds, with four replicates prepared. Error bars indicate SE. Significant differences from the wild type were determined by Student's *t* test (* $P < 0.05$). Dw, Dry weight; Fw, fresh weight.

NO can stimulate the accumulation of both ferritin mRNA and protein, indicating that it is a key signaling molecule for regulating Fe homeostasis in plants (Murgia et al., 2002). Two *ferritin* genes in rice, *OsFer1* and *OsFer2*, show high sequence similarity to each other but distinct expression patterns (Gross et al., 2003). We observed here that transcript levels of both were reduced when Fe was deficient but were elevated by SNP treatment in the wild type and the *osysl15* mutant (Fig. 8A). However, CPTIO diminished this NO effect (Fig. 8B). These results suggest that the mutation in *OsYSL15* did not affect those *ferritin* genes.

Overexpression of *OsYSL15* Using the Rice *Actin* Promoter

We placed *OsYSL15* cDNA in a sense orientation under the control of the rice *Actin1* promoter, resulting in pGA2875 (Fig. 9A). After generating transgenic plants, we studied constitutive expression of that gene using RNA samples prepared from leaves (Fig. 9B). Based on our quantitative real-time PCR analysis, we selected lines 2 (OX-2) and 6 (OX-6) for further examination. Fe and Zn concentrations were measured in their seeds (Fig. 9, C and D) via an atomic absorption spectrometer. Although Fe concentrations in seeds from both transgenic lines were increased compared with the wild type (Fig. 9C), Zn concentrations were not changed by overexpression of *OsYSL15* (Fig. 9D). The levels of Mn and Cu in mature seeds of transgenic plants were similar to those of the wild type (Supplemental Fig. S3, C and D).

Phenotype Analyses of *osysl15-1* Knockout and *OsYSL15* Overexpression Plants Grown under Different Fe Concentrations

Expression of *OsYSL15* was strongly induced by Fe deficiency and was decreased as the Fe concentration increased (Fig. 1). In testing the phenotypes of *osysl15-1* knockout and *OsYSL15*-overexpressing plants, we observed that as the level of Fe rose, chlorophyll concentrations were increased in a dose-dependent manner (Fig. 10). Visual differences were documented by measuring chlorophyll concentrations (Fig. 10B). Under Fe-deficient conditions, the *osysl15-1* knockout plants showed greater chlorosis, but that phenotype disappeared when higher Fe concentrations (at least 100 μM) were supplied. In OX-2 and OX-6 plants, this chlorotic phenotype was diminished at an Fe concentration of 10 μM or greater. These results indicate that

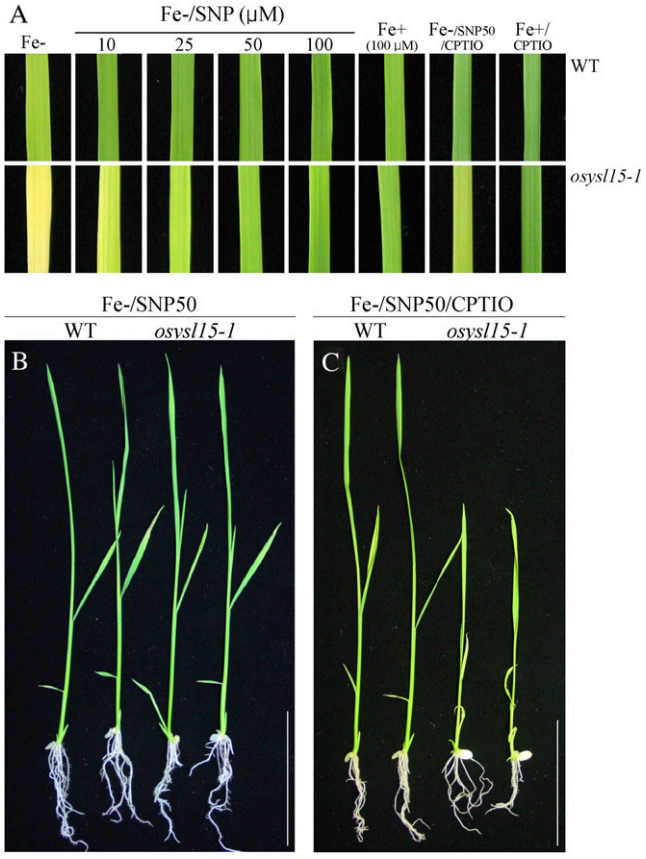

Figure 7. Effect of NO on reversion of chlorosis in the *osysl15-1* mutant. A, Seeds were germinated and plants grown on Fe-sufficient (Fe+) or Fe-deficient (Fe−) medium containing various concentrations of SNP. Photographs were taken from middle sections of second leaves at 10 d after treatment. For NO depletion, 100 μM CPTIO was added to growth medium. B, Phenotypes of 10-d-old plants grown on Fe-deficient medium containing 50 μM SNP. C, Inhibitory effect of CPTIO on NO-treated plants. WT, Wild type. Bars = 5 cm. [See online article for color version of this figure.]

OsYSL15 functions primarily when plants have a low availability of Fe.

Disruption and Overexpression of *OsYSL15* Affects Plant Architecture

To examine how the disruption or overexpression of *OsYSL15* might influence plant architecture and grain yields, we cultivated transgenic seedlings along with their segregated wild-type siblings in the field. All knockout plants as well as OX-2 and OX-6 plants flowered about 10 d later than their wild-type segregants. Whereas transgenic plant heights were significantly reduced (Fig. 11), tiller numbers did not change (Supplemental Table S1). Moreover, although fewer total spikelets were counted on the knockout mutants and overexpression plants, their grain yields were not significantly different from those of the wild type (Supplemental Table S1). We also measured Fe, Zn, Mn, and Cu concentrations in wild-type and mutant flag leaves, sampling for uniformity after flowering. Disruption of *OsYSL15* resulted in reduced Fe levels in flag leaves, while its overexpression increased those values in flag leaves (Fig. 11E). However, Zn, Mn, and Cu concentrations in the flag leaves were unaffected by either disruption or overexpression of *OsYSL15* (Fig. 11F; Supplemental Fig. S3, F and G).

DISCUSSION

Here, we report the functional roles of *OsYSL15* for Fe homeostasis in rice. This was manifested by reduced Fe levels in knockout plants that showed chlorotic phenotypes under Fe deficiency and by increased Fe levels in overexpressors. *OsYSL15* expression was strongly induced by Fe deficiency, suggesting that OsYSL15 is needed when plants grow under such conditions. In roots, this gene was strongly induced in all cell types, including the epidermis, implying that it is involved in Fe uptake from the rhizosphere. The gene was also induced in almost all shoot cell types, except the epidermis, which implies that this transporter functions primarily in distributing Fe. Using a yeast system, we demonstrated that OsYSL15 transports Fe^{3+}-DMA and Fe^{2+}-NA, strongly supporting the possibility of dual roles for OsYSL15: Fe uptake from soil and its distribution in the plant. *OsYSL15* was also expressed in developing seeds, suggesting a role in the translocation of Fe into grains, as confirmed by the reduced Fe concentration in mutant seeds. Furthermore, overexpression of *OsYSL15* resulted in higher Fe concentrations in leaves and seeds, supporting that OsYSL15 is an Fe transporter. Disruption or overexpression of *OsYSL15* affected the concentration of Fe, but not Zn, Mn, or Cu, in our rice plants. Therefore, OsYSL15 appears to be an Fe-specific transporter. Although OsYSL15 is highly homologous to OsYSL2, they appear to have different substrate specificities. OsYSL2 is capable of mediating transport of Fe^{2+}-NA and Mn^{2+}-NA but not Fe^{3+}-DMA and Mn^{2+}-DMA (Koike et al., 2004).

Disruption of *OsYSL15* resulted in a 20% reduction in Fe concentration under both sufficient and deficient conditions. Although no altered phenotypes were visible when Fe supplies were adequate, severe chlorosis occurred in the *osysl15* mutants when Fe was limited. This suggests that OsYSL15 is important for distribution into the chloroplast, as was correlated with a great reduction in chloroplast Fe concentrations. Therefore, how OsYSL15 affects Fe distribution into chloroplasts needs to be investigated.

The disruption or overexpression of *OsYSL15* was manifested by shorter plants and alterations in their architecture. Therefore, because only the concentration of Fe varied, Fe homeostasis must play an important role in growth and development. Because the Fe concentration was altered by such disruption or over-

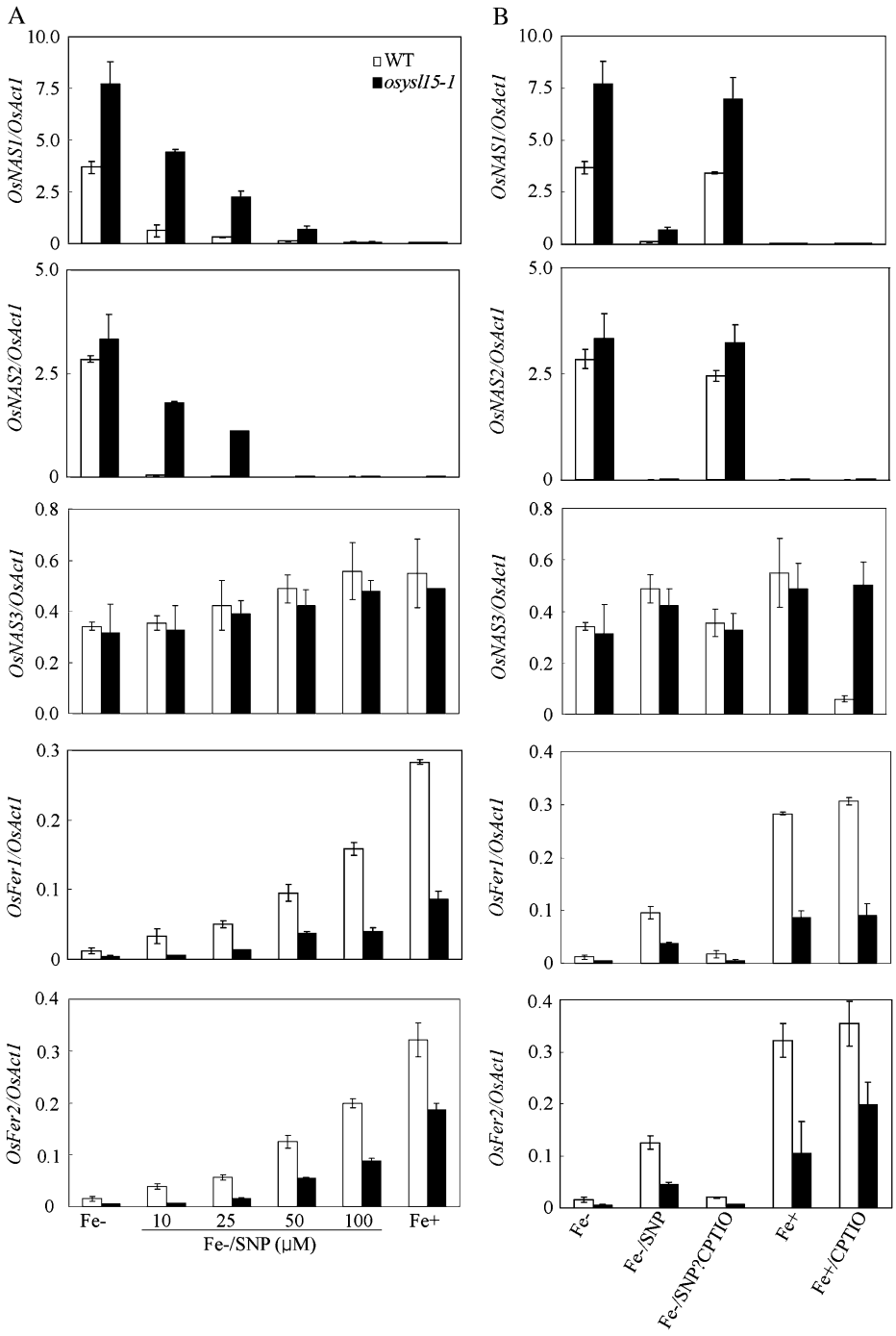

Figure 8. Expression analysis for Fe homeostasis-related genes. RNA was prepared from 10-d-old shoots. A, Real-time PCR analysis of three rice *NAS* genes and two rice *ferritin* genes after SNP treatment. B, Expression analyses of *OsNAS* and *Osferritin* genes in plants grown on medium supplemented with 100 μM CPTIO, an NO inhibitor. Transcript levels are represented by the ratio between mRNA level for *OsNAS* or *Osferritin* genes and that for rice *Actin1*. Error bars indicate SD. WT, Wild type.

expression, the physiological balance of metal ions was disturbed, resulting in defective growth in the field. When *IRT1* is ectopically expressed, transgenic plants show no visible morphological changes (Connolly et al., 2002). Although *IRT1* mRNA is expressed constitutively, IRT1 protein is present only in Fe-limited roots, indicating posttranscriptional regulation of *IRT1* (Vert et al., 2002). Because our *OsYSL15* overexpressors accumulated more Fe and had altered growth, we can assume that OsYSL15 protein levels are higher in the overexpression lines than in the wild types. However, we do not know that posttranscriptional regulation is occurring as AtIRT1. Unfortunately, we were unable to measure the level of OsYSL15 protein due to a lack of available antibodies.

Seedlings of the maize *ys1* mutant, which is defective in the uptake of Fe^{3+}-PS complexes, experience severe Fe deficiency chlorosis (yellowing between the veins) and, ultimately, mortality, indicating that such uptake is an essential process for that species (Walker

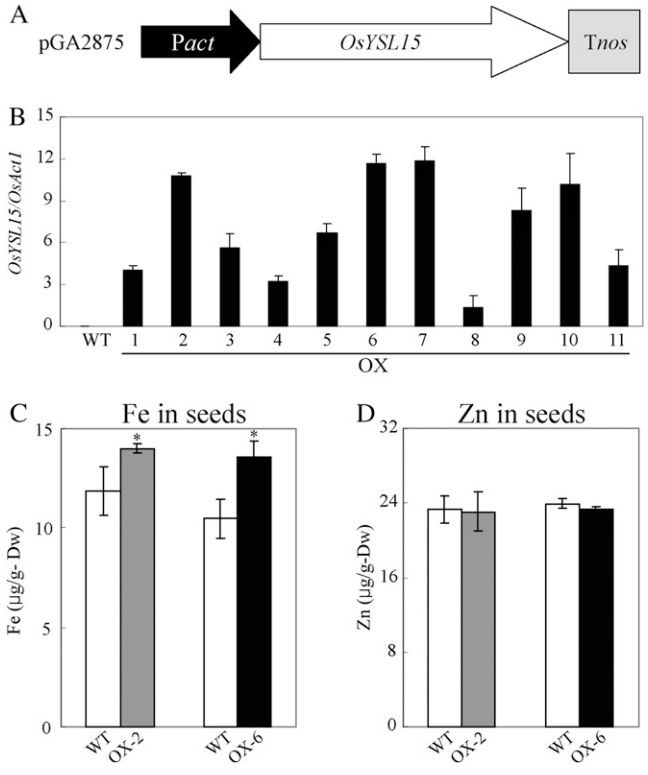

Figure 9. Generation of transgenic plants overexpressing *OsYSL15*. A, Schematic diagram of the pGA2875 construct. *OsYSL15* cDNA was placed between the rice *Actin* promoter (P*act*) and the nopaline synthase terminator (T*nos*). B, Quantitative real-time PCR analysis of overexpression transgenic plants using RNA from leaves. Error bars indicate SD. Transcript levels are represented by the ratio between mRNA level for *OsYSL15* and that for rice *Actin1*. C and D, Fe and Zn concentrations in mature seeds from wild-type and *OsYSL15*-overexpressing (OX-2 and OX-6) plants grown in paddy fields. WT indicates segregated siblings of selected lines. Error bars indicate SE. * $P < 0.05$. Dw, Dry weight.

and Connolly, 2008). Here, however, mutation in *OsYSL15* did not produce lethal phenotypes, although those plants were shorter and contained less Fe, probably because of gene redundancy. Three additional rice genes are highly homologous to maize YS1. Among them, induction patterns for *OsYSL2* and *OsYSL9* by Fe deficiency are quite similar to those for *OsYSL15*. Rice also has efficient Fe^{2+} uptake systems, in contrast to other grasses (Ishimaru et al., 2006).

NO is a bioactive molecule, playing important roles in many physiological processes, including determining Fe availability within a plant (Graziano et al., 2002). Here, we used *osysl15* mutants to evaluate the effect of NO in rice. By treating with SNP, an NO donor, we were able to partially reverse their chlorotic phenotype. An NO scavenger, CPTIO, abolished that protective effect. However, NO treatment did not increase total Fe content within a plant. These results support that NO increases Fe availability in rice, as observed from other organisms. NO stimulates the accumulation of both *ferritin* mRNA and protein in Arabidopsis (Murgia et al., 2002). We observed similar positive effects on rice *ferritin* mRNA levels. In contrast, expression of two *NAS* genes that was induced by Fe deficiency was inhibited by NO. Therefore, we conclude that there are alternative ways to alleviate the stresses associated with diminished supplies of Fe.

Quantitative real-time PCR and promoter-GUS analyses have indicated that *OsYSL15* is strongly induced by lower Fe levels. Two cis-acting elements, IDE1 and IDE2, synergistically mediate Fe deficiency-induced gene expression in tobacco (*Nicotiana tabacum*; Kobayashi et al., 2003). Sequences similar to IDE1 and IDE2 are found in the promoter regions of *OsIRT1*, *OsNAS1*, and *OsNAS2*, which are induced by Fe deficiency (Kobayashi et al., 2003, 2005). The rice basic helix-loop-helix protein OsIRO2, an essential regulator

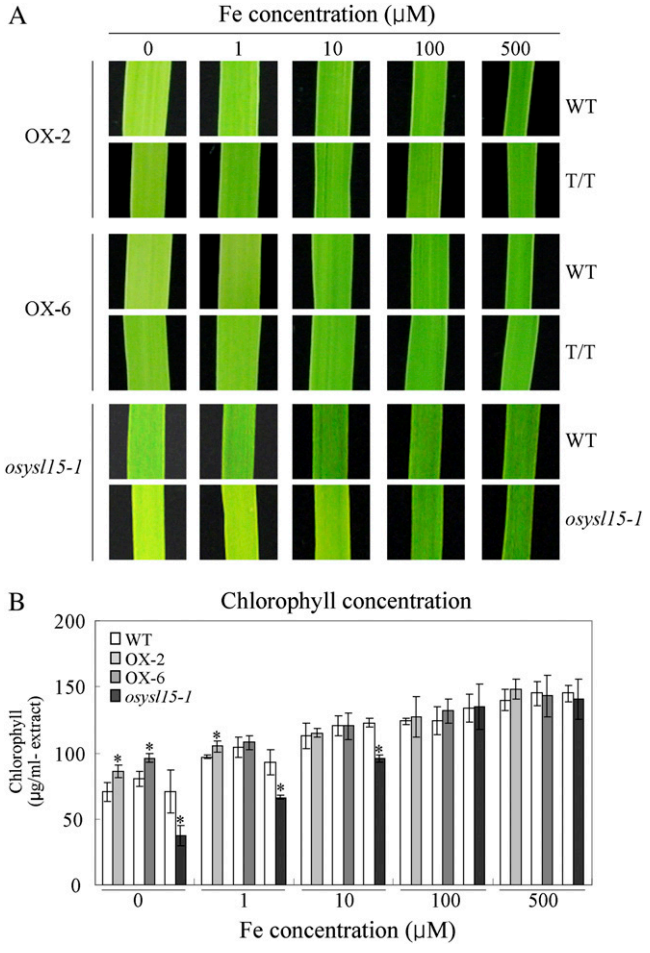

Figure 10. Phenotype analyses of *OsYSL15*-overexpressing transgenic and *osysl15-1* plants grown under different Fe concentrations. A, Representative photographs of second leaves. WT and T/T indicate segregated wild-type and homozygous plants from selected lines. B, Chlorophyll concentrations from plants ($n = 4$) grown at different Fe concentrations. Error bars indicate SE. * $P < 0.05$. [See online article for color version of this figure.]

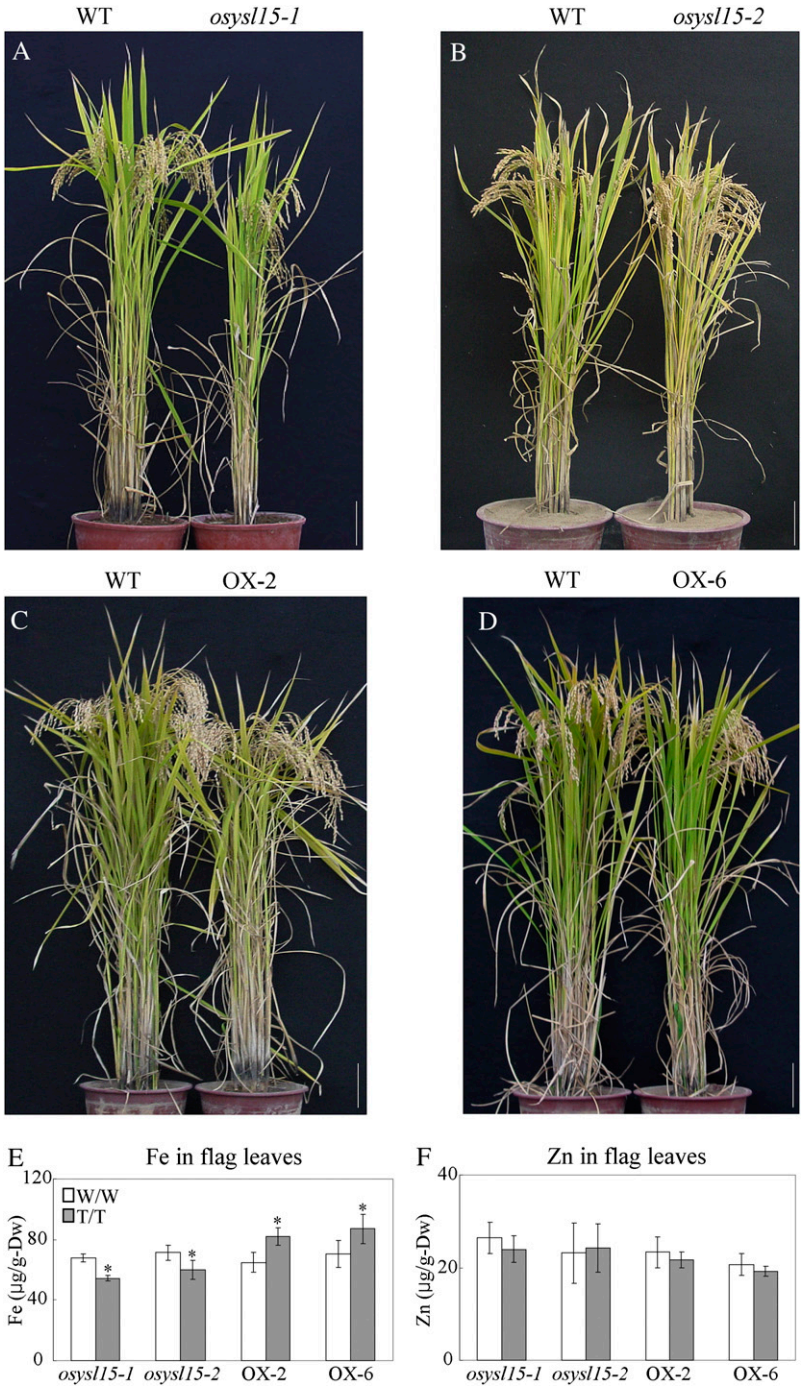

Figure 11. Phenotypes of *OsYSL15* knockout and overexpressing transgenic plants grown in the paddy field. Representative photographs were taken after plants flowered. A and B, Comparisons among wild-type (WT), *osysl15-1*, and *osysl15-2* plants. C and D, Comparison of wild-type and *OsYSL15*-overexpressing (OX-2 and OX-6) plants. For the photographs, transgenic plants were transferred to pots from the paddy fields. Bars = 10 cm. E and F, Fe (E) and Zn (F) concentrations in flag leaves, with each measured from four flag leaves per line sampled after flowering. Error bars indicate SE. * $P < 0.05$. [See online article for color version of this figure.]

of the genes involved in Fe uptake under deficient conditions, also contains putative IDE sequences in its promoter region (Ogo et al., 2006). Therefore, the regulatory networks mediated by IDE elements during Fe deficiency are apparently conserved between dicot and monocot species. The promoter region of *OsYSL15* has two putative IDE sequences, at –249 and –593 bp from the translation initiation site. Our *OsYSL15* promoter-*GUS* construct contained these two putative IDE-like elements, and GUS expression was induced by Fe deficiency. Further research is necessary to verify whether these elements are indeed responsible for that deficiency response. *OsYSL15* is expressed strongly in *OsIRO2*-overexpressing transgenic plants (Ogo et al., 2007), suggesting that the former functions downstream of the latter.

OsYSL15 overexpression was positive in raising the Fe concentration in our seeds and vegetative tissues, albeit with some side effects. This presents the possibility that OsYSL15 can be used for enhancing Fe levels

in rice grains, perhaps via targeted expression with seed-specific promoters.

MATERIALS AND METHODS

Plant Growth

Wild-type transgenic rice (*Oryza sativa* 'Dongjin') and seeds were surface sterilized and germinated on an MS solid medium supplemented with 0, 1, 10, 100, or 500 μM Fe^{3+}-EDTA. Shoot and root samples from 7-d-old seedlings were frozen with liquid nitrogen. SNP (10–100 μM) was used as an NO donor, and 100 μM CPTIO served as an NO scavenger. Transgenic plants were transplanted and grown to maturity in paddy fields located at Pohang University of Science and Technology (36° N). The field tests were performed twice, in 2007 and 2008.

RNA Isolation and RT-PCR Analysis

Total RNA was obtained from each tissue type with an RNA isolation kit (Tri Reagent; MRC). For cDNA synthesis, we used 2 μg of total RNA as template and M-MLV reverse transcriptase (Promega) in a 25-μL reaction mixture. RT-PCR was performed in a 50-μL solution containing a 1-μL aliquot of the cDNA reaction, 0.2 μM gene-specific primers, 10 mM deoxyribonucleotide triphosphates, and 1 unit of rTaq DNA polymerase (Takara Shuzo). PCR products were separated by electrophoresis on a 1.2% agarose gel. Quantitative real-time PCR was performed with a Roche LightCycler II as described previously (Han et al., 2006). The *Actin1* mRNA levels were used to normalize the expression ratio for each gene. Changes in expression were calculated via the $\Delta\Delta_{Ct}$ method. The gene-specific primers are listed in Supplemental Table S2.

Yeast Functional Complementation

RNA was isolated from the roots of 30-d-old rice cv Nipponbare. cDNA was synthesized using the SuperScript First-Strand Synthesis System (Invitrogen) with oligo(dT) primers. RT-PCR was performed with PfuTurbo DNA polymerase (Stratagene) and primers YF (5′-TGCAGCGAATTCTCGAGCAGCTAAGCGAGATCGAC-3′) and YR (5′-TTCTAGAGCGGCCGCCTGCAATCCTCCACCCATGAAAT-3′), which contained *Eco*RI and *Not*I sites (underlined sequences) for cloning, respectively. The resulting product was ligated into the *Not*I/*Eco*RI-digested pYES6/CT vector. *Saccharomyces cerevisiae* strain DEY1453 (*MATa/MATa ade2/ADE2 can1/can1 his3/his3 leu2/leu2 trp1/trp1 ura3/ura3 fet3-2::HIS3/fet3-2::HIS3 fet4-1::LEU2/fet4-1::LEU2*) was transformed with pGEV-Trp (Gao and Pinkham, 2000) together with *pYES6/CT* or *pYES6/CT* expressing *OsYSL15*.

For complementation assays, synthetic dextrose (SD)-Trp medium was made with an Fe-free yeast nitrogen base buffered with 25 mM MES at pH 5.7 for plates containing Fe^{2+} or at pH 6.0 for plates containing Fe^{3+}. To prepare our Fe^{2+} assay, the following were added, in order, to the center of each empty plate: 125 μL of 200 mM ascorbic acid, 7.5 μL of freshly prepared 10 mM Fe_2SO_4, and 20 μL of 10 mM NA. This solution was mixed briefly and then incubated at room temperature for 10 min to allow complex formation. Afterward, 25 mL of molten SD-Trp with 10 μg mL^{-1} blasticidin was added, which was then allowed to solidify. To prepare for our Fe^{3+} assay, 34 μL of 7.4 mM $FeCl_3$ and 25 μL of 10 mM DMA were placed in the center of each empty plate and incubated at room temperature for 10 min. We then added 25 mL of molten SD-Trp with 10 μg mL^{-1} blasticidin to the plates before solidification. To prepare plates with 10 mM BPDS, 25 μL was incorporated just prior to the addition of the molten medium.

Suspensions were prepared from 3-d-old yeast colonies, which were removed from the plates and suspended in sterile water before the optical density at 550 nm of the resulting suspension was measured. After that value was brought to 0.1, serial dilutions (1:10, 1:100, 1:1,000, and 1:10,000) of the suspension were prepared, and 7 μL of each dilution was spotted on the plates. They were then grown at 28°C for 3 d.

Generation of the *OsYSL15* Promoter-*GUS* Fusion Molecule and GUS Assay

Genomic sequences (–1,000 to –1 bp from the translation initiation site) containing the promoter region of *OsYSL15* were amplified by PCR using two primers (pf, 5′-AAAAGCTTAGCATGTCTCCAGATTCTCCAT-3′; and pr, 5′-AAGGATCCGCGGCGGCGGCGGCGTCGATCTC-3′). This fragment was connected to a *GUS-NOSt* cassette (derived from pBI101.2) and ligated into pCAMBIA1302, resulting in pGA2866. This plasmid was transferred to *Agrobacterium tumefaciens* strain LBA4404 by the freeze-thaw method (An et al., 1988), and transgenic plants carrying the above construct were generated via *Agrobacterium*-mediated cocultivation (Lee et al., 1999). Histochemical GUS staining of those transgenic plants was performed according to the method reported by Dai et al. (1996). Ten-micrometer sections were prepared as described previously by Jung et al. (2005) and were observed with a microscope (Nikon) under bright-field illumination.

Subcellular Localization of the OsYSL15-GFP Fusion Protein in Onion Epidermal Cells

Full-length *OsYSL15* cDNA was PCR amplified with the primer pair gf (5′-AATCTAGAGTTTCTTTCTTGTCCTCGTGGT-3′) and gr (5′-AAGGATCCAGCTTCCAGGCGTAAACTTCATGC-3′). These primers contained *Xba*I or *Bam*HI sites (underlined sequences) to facilitate cloning of the amplified cDNA. After sequence analysis, the *OsYSL15* cDNA was cloned into the *Xba*I and *Bam*HI sites of the 326-GFP vector (Lee et al., 2001). The AHA2-RFP fusion molecule under the control of the cauliflower mosaic virus *35S* promoter was obtained from Inhwan Hwang (Pohang University of Science and Technology). Constructs were introduced into onion (*Allium cepa*) epidermal cells by particle bombardment using the Biolistic PDS-1000/He particle delivery system (Bio-Rad). At 12 h after transformation, expression of GFP and RFP was monitored with a fluorescence microscope and two filters (Axioplan2; Carl Zeiss).

Isolation of *OsYSL5* Loss-of-Function Plants

Two putative *OsYSL15* knockout mutants were isolated from our rice flanking sequence tag database (http://www.postech.ac.kr/life/pfg). T2 progeny of the primary mutants were grown to maturity to amplify their seeds. Genotyping of these progeny was determined by PCR using three primers. These included the following: for *osysl15-1* (line 2D-10712), two specific primers (F1, 5′-GCCTTTCTTCCCTTAATTTGATCCAC-3′; and R1, 5′-CTTAACAAATCTATACTGCTTT-3′) and one T-DNA-specific primer (LB; 5′-ACGTCCGCAATGTGTTATTAA-3′); for *osysl15-2* (line 3A-10357), two specific primers (F2, 5′-ATAGGCAGAGGGTTCCATTT-3′; and R2, 5′-AGCCACCTCACACAAGAGAG-3′) and a T-DNA-specific primer (LB; 5-ACGTCCGCAATGTGTTATTAA-3′). Afterward, transcript levels for *OsYSL15* were determined by RT-PCR using cDNA prepared from the leaves of 10-d-old seedlings grown under Fe deficiency.

Generation of the *OsYSL15*-Overexpressing Construct

To create our *OsYSL15*-overexpressing construct, the full-length cDNA sequence of *OsYSL15* was amplified by a primer pair (FL, 5′-AATCTAGAGTTTCTTTCTTGTCCTCGTGGT-3′; and RL, 5′-AACTCGAGACCTCTTAGCTTCCAGGCGTAA-3′). The PCR product was cloned into *Xba*I and *Xho*I sites between the rice *Actin1* promoter (McElroy et al., 1990) and the *T7* terminator of the binary vector pGA1671, thereby generating pGA2875 (Jeon et al., 2000). Transformation of this plasmid into *Agrobacterium* and the generation of transgenic plants were as described previously (Lee et al., 1999).

Preparation of Protoplast and Chloroplast

Mesophyll protoplasts were prepared as described previously by Moon et al. (2008). Briefly, the third leaves were harvested and dissected from 10-d-old seedlings grown on either MS or Fe-deficient medium. The materials were digested in an enzyme solution (1.5% cellulase RS, 0.3% macerozyme, 0.1% pectolyase, 0.6 M mannitol, 10 mM MES, 1 mM $CaCl_2$, and 0.1% [w/v] bovine serum albumin) for 4 h at 26°C with gentle agitation (50–75 rpm). KMC solution (117 mM KCl, 82 mM $MgCl_2$, and 85 mM $CaCl_2$) was added afterward. Protoplasts were sorted from the debris through a nylon mesh (20 μm), collected by centrifuging at 1,000 rpm for 2 min, and resuspended in EP3 solution (70 mM KCl, 5 mM $MgCl_2$, 0.4 M mannitol, and 0.1% MES, pH 5.6). Chloroplasts were isolated according to the published protocol (Triboush et al., 1998). Five grams of leaves from 10-d-old seedlings was homogenized in a mortar with 20 mL of STE buffer (400 mM Suc, 50 mM Tris, pH 7.8, 20 mM

EDTA-Na_2, 0.2% bovine serum albumin, and 0.2% β-mercaptoethanol). After the homogenate was filtered through a 50-μm nylon mesh, the extract was centrifuged at 1,000 rpm. The supernatant was then centrifuged at 4,000 rpm, and this resuspended pellet was centrifuged again at 4,000 rpm to prepare the chloroplast fraction.

Measurement of Plant Growth and Metal Concentrations

Seeds of the wild type and mutant were germinated, and plants were then grown for 10 d on a solid medium containing MS salts supplemented with different concentrations of Fe^{3+}-EDTA. Their chlorophyll concentrations were measured as described previously (Lee et al., 2005). Briefly, 0.1 g of leaf samples was harvested and the chlorophyll was extracted with 1 mL of 80% acetone. After homogenization, the samples were incubated for 15 min and spun at 15,000*g* for 10 min before an aliquot of the supernatant fraction was taken to measure A_{663} and A_{643} with a spectrophotometer. Chlorophyll concentrations, including chlorophyll *a* and *b*, were determined according to the method of Arnon (1949), and metal concentrations were measured as described previously by Kim et al. (2002). Seeds and shoot and root portions were dried for 2 d at 70°C before those samples were weighed. Afterward, they were digested in 1 mL of 11 N HNO_3 for 3 d at 200°C. Following dilution, their metal concentrations were determined by an atomic absorption spectrometer (SpectrAA-800; Varian).

Sequence data from this article can be found in the GenBank/EMBL data libraries under accession numbers number AB190923.

Supplemental Data

The following materials are available in the online version of this article.

Supplemental Figure S1. Expression analyses of *OsYSL* genes that were constitutive under different iron concentrations.

Supplemental Figure S2. Quantification of wild type and *osysl15* mutants grown on control MS (100 μM Fe and 30 μM Zn), Fe-deficient (Fe−), or Zn-deficient (Zn−) medium for 10 d following germination.

Supplemental Figure S3. Mn and Cu concentrations in wild-type and transgenic plants.

Supplemental Figure S4. Characterization of wild-type and *osysl15-1* mutant plants grown with various concentrations of SNP.

Supplemental Table S1. Characterization of *osysl15* mutants grown in the paddy field.

Supplemental Table S2. Primers used for RT-PCR analysis.

ACKNOWLEDGMENTS

We thank Inhwan Hwang for providing AtAHA2:RFP, In-Soon Park and Kyungsook An for plant transformation, Jongdae Kyung for technical assistance with the atomic absorption spectrometer measurements, Changduk Jung for growing plants, and Priscilla Licht for critical reading of the manuscript.

Received January 8, 2009; accepted April 14, 2009; published April 17, 2009.

LITERATURE CITED

An G, Ebert PR, Mitra A, Ha SB (1988) Binary vectors. *In* SB Gelvin, RA Schilperoort, eds, Plant Molecular Biology Manual. Kluwer Academic Publishers, Dordrecht, The Netherlands, pp A3/1–A3/19

An S, Park S, Jeong DH, Lee DY, Kang HG, Yu JH, Hur J, Kim SR, Kim YH, Lee M, et al (2003) Generation and analysis of end sequence database for T-DNA tagging lines in rice. Plant Physiol **133:** 2040–2047

Anbar M (1995) Nitric oxide: a synchronizing chemical messenger. Experientia **51:** 545–550

Arnon DI (1949) Copper enzymes in isolated chloroplasts: polyphenoloxidase in *Beta vulgaris*. Plant Physiol **24:** 1–15

Bashir K, Inoue H, Nagasaka S, Takahashi M, Nakanishi H, Mori S, Nishizawa NK (2006) Cloning and characterization of deoxymugineic acid synthase genes from graminaceous plants. J Biol Chem **281:** 32395–32402

Beligni MV, Lamattina L (2001) Nitric oxide: a non-traditional regulator of plant growth. Trends Plant Sci **6:** 508–509

Bughio N, Yamaguchi H, Nishizawa NK, Nakanishi H, Mori S (2002) Cloning an iron-regulated metal transporter from rice. J Exp Bot **53:** 1677–1682

Connolly EL, Fett JP, Guerinot ML (2002) Expression of the IRT1 metal transporter is controlled by metals at the levels of transcript and protein accumulation. Plant Cell **14:** 1347–1357

Curie C, Panaviene Z, Loulergue C, Dellaporta SL, Briat JF, Walker EL (2001) Maize *yellow stripe1* encodes a membrane protein directly involved in Fe (III) uptake. Nature **409:** 346–349

Dai Z, Gao J, An K, Lee JM, Edwards GE, An G (1996) Promoter elements controlling developmental and environmental regulation of a tobacco ribosomal protein L34. Plant Mol Biol **32:** 1055–1065

DiDonato RJ Jr, Roberts LA, Sanderson T, Eisley RB, Walker EL (2004) *Arabidopsis Yellow Stripe-Like2* (*YSL2*): a metal-regulated gene encoding a plasma membrane transporter of nicotianamine-metal complexes. Plant J **39:** 403–414

Dix DR, Bridgham JT, Broderius MA, Byersdorfer CA, Eide DJ (1994) The FET4 gene encodes the low affinity Fe(II) transport protein of *Saccharomyces cerevisiae*. J Biol Chem **269:** 26092–26099

Durner J, Klessig DF (1999) Nitric oxide as a signal in plants. Curr Opin Plant Biol **2:** 369–374

Eide D, Broderius M, Fett J, Guerinot ML (1996) A novel iron regulated metal transporter from plants identified by functional expression in yeast. Proc Natl Acad Sci USA **93:** 5624–5628

Gao CY, Pinkham JL (2000) Tightly regulated, beta-estradiol dose-dependent expression system for yeast. Biotechniques **29:** 1226–1231

Gendre D, Czernic P, Conéjéro G, Pianelli K, Briat J-F, Lebrun M, Mari S (2007) *TcYSL3*, a member of the YSL gene family from the hyperaccumulator *Thlaspi caerulescens*, encodes a nicotianamine-Ni/Fe transporter. Plant J **49:** 1–15

Graziano M, Beligni MV, Lamattina L (2002) Nitric oxide improves internal iron availability in plants. Plant Physiol **130:** 1852–1859

Graziano M, Lamattina L (2005) Nitric oxide and iron in plants: an emerging and converging story. Trends Plant Sci **10:** 4–8

Graziano M, Lamattina L (2007) Nitric oxide accumulation is required for molecular and physiological responses to iron deficiency in tomato roots. Plant J **52:** 949–960

Gross J, Stein JS, Fett-Neto AG, Fett JP (2003) Iron homeostasis related genes in rice. Genet Mol Biol **26:** 477–497

Han MJ, Jung KH, Yi G, Lee DY, An G (2006) Rice immature pollen 1 (RIP1) is a regulator of late pollen development. Plant Cell Physiol **47:** 1457–1472

Henriques R, Jasik J, Klein M, Martinoia E, Feller U, Schell J, Pais MS, Koncz C (2002) Knock-out of *Arabidopsis* metal transporter gene *IRT1* results in iron deficiency accompanied by cell differentiation defects. Plant Mol Biol **50:** 587–597

Higuchi K, Suzuki K, Nakanishi H, Yamaguchi H, Nishizawa NK, Mori S (1999) Cloning of nicotianamine synthase genes, novel genes involved in the biosynthesis of phytosiderophores. Plant Physiol **119:** 471–480

Inoue H, Higuchi K, Nakanishi H, Mori S, Nishizawa NK (2003) Three rice nicotianamine synthase genes, *OsNAS1, OsNAS2* and *OsNAS3*, are expressed in cells involved in long-distance transport of iron and differentially regulated by iron. Plant J **36:** 366–381

Inoue H, Kobayashi T, Nozoye T, Takahashi M, Kakei Y, Suzuki K, Nakazono M, Nakanishi H, Mori S, Nishizawa NK (2009) Rice OsYSL15 is an iron-regulated iron(III)-deoxymugineic acid transporter expressed in the roots and is essential for iron uptake in early growth of the seedlings. J Biol Chem **284:** 3470–3479

Inoue H, Takahashi M, Kobayashi T, Suzuki M, Nakanishi H, Mori S, Nishizawa NK (2008) Identification and localisation of the rice nicotianamine aminotransferase gene OsNAAT1 expression suggests the site of phytosiderophore synthesis in rice. Plant Mol Biol **66:** 193–203

Ishimaru Y, Suzuki M, Tsukamoto T, Suzuki K, Nakazono M, Kobayashi T, Wada Y, Watanabe S, Matsuhashi S, Takahashi M, et al (2006) Rice plants take up iron as an Fe^{3+}-phytosiderophore and as Fe^{2+}. Plant J **45:** 335–346

Jeon JS, Jang S, Lee S, Nam J, Kim C, Lee SH, Chung YY, Kim SR, Lee YH, Cho YG, et al (2000) *leafy hull sterile1* is a homeotic mutation in a rice

MADS box gene affecting rice flower development. Plant Cell **12:** 871–884

Jeong DH, An S, Park S, Kang HG, Park GG, Kim SR, Sim J, Kim YO, Kim MK, Kim SR, et al (2006) Generation of a flanking sequence-tag database for activation-tagging lines in japonica rice. Plant J **45:** 123–132

Jung KH, Han MJ, Lee YS, Kim YW, Hwang I, Kim MJ, Kim YK, Nahm BH, An G (2005) *Rice Undeveloped Tapetum1* is a major regulator of early tapetum development. Plant Cell **17:** 2705–2722

Kim DH, Eu YJ, Yoo CM, Kim YW, Pih KT, Jin JB, Kim SJ, Stenmark H, Hwang I (2001) Trafficking of phosphatidylinositol 3-phosphate from the trans-Golgi network to the lumen of the central vacuole in plant cells. Plant Cell **13:** 287–301

Kim YY, Yang YY, Lee Y (2002) Pb and Cd uptake in rice roots. Physiol Plant **116:** 368–372

Kobayashi T, Nakayama Y, Nakanishi-Itai R, Nakanishi H, Yoshihara T, Mori S, Nishizawa NK (2003) Identification of novel cis-acting elements, IDE1 and IDE2, of the barley IDS2 gene promoter conferring iron-deficiency-inducible, root-specific expression in heterogeneous tobacco plants. Plant J **36:** 780–793

Kobayashi T, Suzuki M, Inoue H, Itai RN, Takahashi M, Nakanishi H, Mori S, Nishizawa NK (2005) Expression of iron-acquisition-related genes in iron-deficient rice is coordinately induced by partially conserved iron-deficiency-responsive elements. J Exp Bot **56:** 1305–1316

Koike S, Inoue H, Mizuno D, Takahashi M, Nakanishi H, Mori S, Nishizawa NK (2004) OsYSL2 is a rice metal-nicotianamine transporter that is regulated by iron and expressed in the phloem. Plant J **39:** 415–424

Lamattina L, Garcia-Mata C, Graziano M, Pagnussat G (2003) Nitric oxide: the versatility of an extensive signal molecule. Annu Rev Plant Biol **54:** 109–136

Lee S, Jeon JS, Jung KH, An G (1999) Binary vector for efficient transformation of rice. J Plant Biol **42:** 310–316

Lee S, Kim JH, Yoo ES, Lee CH, Hirochika H, An G (2005) Differential regulation of *chlorophyll a oxygenase* genes in rice. Plant Mol Biol **57:** 805–818

Lee YJ, Kim DH, Kim YW, Hwang I (2001) Identification of a signal that distinguishes between the chloroplast outer envelope membrane and the endomembrane system in vivo. Plant Cell **13:** 2175–2190

Le Jean M, Schikora A, Mari S, Briat JF, Curie C (2005) A loss-of-function mutation in *AtYSL1* reveals its role in iron and nicotianamine seed loading. Plant J **44:** 769–782

Lopez-Bucio J, Acevedo-Hernandez G, Ramirez-Chavez E, Molina-Torres J, Herrera-Estrella L (2006) Novel signals for plant development. Curr Opin Plant Biol **9:** 523–529

Marschner H, Romheld V, Kissel M (1986) Different strategies in higher plants in mobilization and uptake of iron. J Plant Nutr **9:** 3–7

McElroy D, Zhang W, Cao J, Wu R (1990) Isolation of an efficient actin promoter for use in rice transformation. Plant Cell **2:** 163–171

Moon S, Giglione C, Lee DY, An S, Jeong DH, Meinnel T, An G (2008) Rice peptide deformylase PDF1B is crucial for development of chloroplasts. Plant Cell Physiol **49:** 1536–1546

Murgia I, Delledonne M, Soave C (2002) Nitric oxide mediates iron-induced ferritin accumulation in *Arabidopsis*. Plant J **30:** 521–528

Neill SJ, Desikan R, Clarke A, Hurst RD, Hancock JT (2002) Hydrogen peroxide and nitric oxide as signalling molecules in plants. J Exp Bot **53:** 1237–1247

Ogo Y, Itai RN, Nakanishi H, Inoue H, Kobayashi T, Suzuki M, Takahashi M, Mori S, Nishizawa NK (2006) Isolation and characterization of IRO2, a novel iron-regulated bHLH transcription factor in graminaceous plants. J Exp Bot **57:** 2867–2878

Ogo Y, Nakanishi Itai R, Nakanishi H, Kobayashi T, Takahashi M, Mori S, Nishizawa NK (2007) The rice bHLH protein OsIRO2 is an essential regulator of the genes involved in Fe uptake under Fe-deficient conditions. Plant J **51:** 366–377

Roberts LA, Pierson AJ, Panaviene Z, Walker EL (2004) Yellow-stripe1: expanded roles for the maize iron-phytosiderophore transporter. Plant Physiol **135:** 112–120

Robinson NJ, Procter CM, Connolly EL, Guerinot ML (1999) A ferric-chelate reductase for iron uptake from soils. Nature **397:** 694–697

Schaaf G, Ludewig U, Erenoglu BE, Mori S, Kitahara T, von Wirén N (2004) ZmYS1 functions as a proton-coupled symporter for phytosiderophore- and nicotianamine-chelated metals. J Biol Chem **279:** 9091–9096

Schaaf G, Schikora A, Haberle J, Vert G, Ludewig U, Briat JF, Curie C, von Wiren N (2005) A putative function for the *Arabidopsis* Fe-phytosiderophore transporter homolog AtYSL2 in Fe and Zn homeostasis. Plant Cell Physiol **46:** 762–774

Takagi SI, Nomoto K, Takemoto T (1984) Physiological aspect of mugineic acid, a possible phytosiderophore of graminaceous plants. J Plant Nutr **7:** 1–5

Takahashi M, Yamaguchi H, Nakanishi H, Shioiri T, Nishizawa NK, Mori S (1999) Cloning two genes for nicotianamine aminotransferase, a critical enzyme in iron acquisition (strategy II) in graminaceous plants. Plant Physiol **121:** 947–956

Takizawa R, Nishizawa NK, Nakanishi H, Mori S (1996) Effect of iron deficiency on *S*-adenosylmethionine synthetase in barley roots. J Plant Nutr **19:** 1189–1200

Triboush SO, Danilenko NG, Davydenko OG (1998) A method for isolation of chloroplast DNA and mitochondrial DNA from sunflower. Plant Mol Biol Rep **16:** 183–189

Varotto C, Maiwald D, Pesaresi P, Jahns P, Salamini F, Leister D (2002) The metal ion transporter IRT1 is necessary for iron homeostasis and efficient photosynthesis in *Arabidopsis thaliana*. Plant J **31:** 589–599

Vert G, Grotz N, Dedaldechamp F, Gaymard F, Guerinot ML, Briat JF, Curie C (2002) IRT1, an *Arabidopsis* transporter essential for iron uptake from the soil and for plant growth. Plant Cell **14:** 1223–1233

von Wirén N, Klair S, Bansal S, Briat JF, Khodr H, Shioiri T, Leigh RA, Hider RC (1999) Nicotianamine chelates both FeIII and FeII: implications for metal transport in plants. Plant Physiol **119:** 1107–1114

Walker EL (2002) Functional analysis of the *Arabidopsis* yellow stripe-like (YSL) family: heavy metal transport and partitioning via metal-nicotianamine (NA) complexes. Plant Physiol **129:** 431–432

Walker EL, Connolly E (2008) Time to pump iron: iron-deficiency-signaling mechanisms of higher plants. Curr Opin Plant Biol **11:** 530–535

Waters BM, Chu HH, Didonato RJ, Roberts LA, Eisley RB, Lahner B, Salt DE, Walker EL (2006) Mutations in Arabidopsis *yellow stripe-like1* and *yellow stripe-like3* reveal their roles in metal ion homeostasis and loading of metal ions in seeds. Plant Physiol **141:** 1446–1458

World Health Organization (2003) Iron deficiency anaemia. http://www.who.int/nutrition/topics/ida/en/index.html (May 1, 2009)

Zaharieva T, Romheld V (2001) Specific Fe^{2+} uptake system in strategy I plants inducible under Fe deficiency. J Plant Nutr **23:** 1733–1744